



ORIGINAL ARTICLE

Metabolites identification of oil palm roots infected with *Ganoderma boninense* using GC–MS-based metabolomics



Azizul Isha^{a,*}, Nor Azah Yusof^{b,c,*}, Khozirah Shaari^{a,b}, Rosiah Osman^c, Siti Nor Akmar Abdullah^d, Mui-Yun Wong^d

^a Laboratory of Natural Products, Institute of Bioscience, Universiti Putra Malaysia, 43400 UPM Serdang, Selangor, Malaysia

^b Department of Chemistry, Faculty of Science, Universiti Putra Malaysia, 43400 UPM Serdang, Selangor, Malaysia

^c Functional Devices Laboratory, Institute of Advanced Technology, Universiti Putra Malaysia, 43400 UPM Serdang, Selangor, Malaysia

^d Institute of Plantation Studies, Universiti Putra Malaysia, 43400 UPM Serdang, Selangor, Malaysia

Received 2 December 2019; accepted 19 May 2020

Available online 29 May 2020

KEYWORDS

Ganoderma boninense;
GC–MS;
Metabolomics;
Oil palm roots;
Principal component analysis

Abstract An approach to metabolomics profiling of non-infected and *Ganoderma boninense* (*G. boninense*) infected oil palm roots crude extracts that utilize gas chromatography-mass spectrometry (GC–MS) and multivariate statistics of principal component analysis (PCA) have been tested. This combination has provided a rapid approach in investigating the changes in the metabolite variations of non-infected and infected oil palm roots at 14 and 30 days post-infection. The extracts were prepared by using 80% (v/v) of methanol. In identifying the metabolites responsible for each differentiation, PCA model was generated in loading bi-plot. Dimethyl benzene-1,4-dicarboxylate, methyl 3-(3,5-ditert-butyl-4-hydroxyphenyl)propanoate, ergost-5-en-3-ol, (3 β), stigmast-5-en-3-ol, (3 β), stigmasterol, methyl hexadecanoate, methyl (9Z,12Z)-octadeca-9,12-dienoate, methyl octadecanoate, 2-(hydroxymethyl)-2-nitropropane-1,3-diol, methyl (Z)-octadec-6-enoate and (E)-icos-5-ene were found more abundant in *G. boninense* infected roots than in non-infected roots. Steroidal

* Corresponding authors at: Laboratory of Natural Products, Institute of Bioscience, Universiti Putra Malaysia, 43400 UPM Serdang, Selangor Malaysia (A. Isha); Functional Devices Laboratory, Institute of Advanced Technology, Universiti Putra Malaysia, 43400 UPM Serdang, Selangor Malaysia (N.A. Yusof).

E-mail addresses: azizul_isha@upm.edu.my (A. Isha), azahy@upm.edu.my (N.A. Yusof).

Peer review under responsibility of King Saud University.



compounds and fatty acid derivatives which has been determined in the non-infected and *G. boninense* infected roots regulate a variety of responses to the *G. boninense*. The abundant of these metabolites in *G. boninense* infected roots are due to the crucial roles in pathogen defence.

© 2020 The Author(s). Published by Elsevier B.V. on behalf of King Saud University. This is an open access article under the CC BY-NC-ND license (<http://creativecommons.org/licenses/by-nc-nd/4.0/>).

1. Introduction

Ganoderma boninense (*G. boninense*), is as a major threat to the lucrative palm oil industry which causes both basal stem rot and upper stem rot of oil palm (*Elaeis Guineensis* Jacq.) It affects the direct loss of stand and reduction of yield of diseased palms (Flood et al. 2002, Hushiarian et al., 2013). The problem and challenge to control the disease come from the characteristics of *G. boninense*. It has been reported that the fungus is soil borne. The fungicides may be ineffective due to degradation in the soil before they can get to their target. It also has various mode of resting stages such as resistant mycelium, basidiospores, chlamyospores and pseudosclerotia (Muniroh et al., 2019; Susanto et al., 2005).

Plant metabolomics, an important tool for investigations of system biology. It has been used to identify the entire profile of detectable metabolites contained in a biological system. (Rozali et al., 2017) has studied the *G. boninense* infected oil palm leaf using two-dimensional gas chromatography coupled with time-of-flight mass spectrometry (GCxGC-TOF-MS) based on metabolomics approach. Their finding revealed that, mannose, xylose, glucopyranose, myo-inositol and hexadecanoic acid were found higher in partially tolerant oil palm whereas cadaverine and turanose were more abundant in susceptible oil palm after conducted partial least squares-discriminant analysis (PLS) and orthogonal partial least squares-discriminant analysis (OPLS-DA).

Determination of aqueous methanolic extract of parental palms root tissues that are partially tolerant and susceptible to *G. boninense* using liquid chromatography-mass spectrometry (LC-MS) has been done by (Zain et al., 2013). Nine metabolites which are broad range of sugars and phenolics derivatives such as sedoheptulose, procyanidin B1, procyanidin B isomer, pinocembrin malonylhexoside, hydroxy-dimethoxybenzoyl-sulfo-hexoside, dimethoxyphenyl-*O*-hexose-*O*-pentoside, trimethoxyphenyl-*O*-hexose-*O*-pentoside, dimethoxybenzyl-*O*-hexose-*O*-rhamnoside and dimethoxyphenylethyl-*O*-hexose-*O*-rhamnoside were determined in their study.

Gas chromatography-mass spectrometry (GC-MS) is an effective system with a highly sensitive and high-throughput analytical platform which has been demonstrated a beneficial tool for untargeted studies of primary metabolism in a several of fields (Durak & Genel, 2020; Durak et al., 2019; Zhou et al., 2020). Application of metabolomics approach in GC-MS requires a multistep procedure which include standardization of an untargeted GC-MS metabolomics protocol such as integrated optimization of pre-analytical, analytical and computational steps.

Metabolites in plants have a critical role in the interaction between host and pathogens (Hu et al., 2019; Karre et al., 2017; Kumar et al., 2016; Yogendra et al., 2015). The changes in metabolism caused by the interaction between *G. boninense*

and oil palm roots are not yet clear. In this work, a comparative metabolome method based on GC-MS was applied to non-infected and *G. boninense*-infected oil palm roots to determine for biomarkers associated with pathogen infection and to setup a diagnostic PCA method. The aim was to further understand the interaction mechanism between *G. boninense* and oil palm roots and provide technical support for the early diagnosis of *G. boninense* disease in oil palm.

2. Materials and methods

2.1. Plant materials and sample preparation

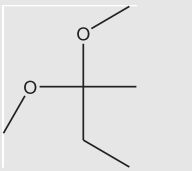
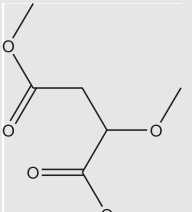
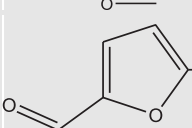
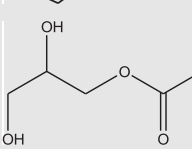
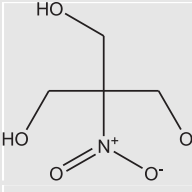
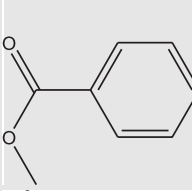
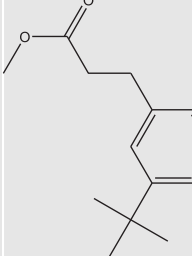
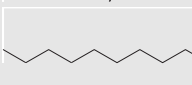
Plant materials used and preparation of samples were conducted according to our previous work reported in detection of *G. boninense* infected oil palm leaf (Isha et al., 2019). Three months old Commercial DxP GH500 germinated seedlings from Sime Darby Seeds & Agricultural Services Sdn. Bhd., Banting were used in this study.

Ten germinated seedlings were treated with *G. boninense* inoculated rubber wood blocks (RWBs) whereas ten germinated seedlings without any treatments of RWBs were used as control. RWB method was prepared based on the method described by Idris et al., 2006. *G. boninense* PER 71 cultures were provided by stock collection of Department of Plant Protection, Faculty of Agriculture, Universiti Putra Malaysia. They were maintained onto potato dextrose agar (Difco Laboratories, Detroit, Michigan, USA) and incubated at 27 ± 1 °C for 7 days. RWBs of 6 cm × 6 cm × 6 cm in size were used as a source of inoculum for fungal colonization. The RWBs were sterilized and autoclaved at 121 °C for 15 min. Each RWB was placed in a heat-resistant polypropylene bag containing 120 mL of malt extract broth and autoclaved at 121 °C for 15 min. Then the bags were left to solidify. Mature *G. boninense* plate cultures (cut into smaller pieces) were inoculated into the RWBs and incubated in the dark until the blocks were fully colonized.

For treatment seedlings, germinated seedlings were placed on top of the RWB and filled with more soil. Root sample were harvested at 14 and 30 days post-infection. Each root sample was quenched with liquid nitrogen and ground into powder form. Freeze-dry system (Scanvac Labogene) was used to remove the water content in the samples. Cultivation took place at the Transgenic Green House, Institute of Plantation Studies, UPM under control conditions.

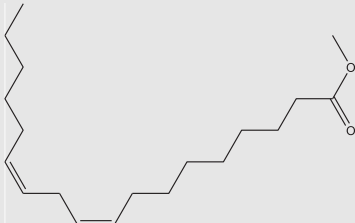
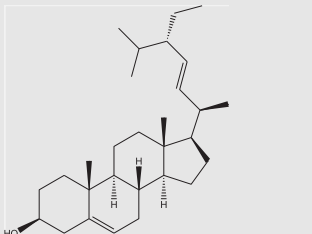
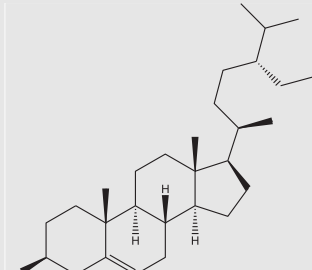
The freeze-dried roots powder of non-infected and *G. boninense* infected oil palm (150 mg) were extracted in 250 mL 80% commercial-grade methanol (30 min, 40 °C) using sonicator. The residue was reextracted twice with the same procedure and the total combined supernatant was filtered through Whatman filter paper (125 mm). The supernatant was evaporated to dryness in a rotary evaporator. The crude extracts obtained were stored at -80 °C until further use.

Table 1 Chemical composition of healthy roots (control of 14 days-post infection) and *G. boninense* infected roots at 14 days-post infection.

Metabolites	Structure	Healthy roots		<i>G. boninense</i> infected roots	
		Concentration (%)	Retention Time (RT)	Concentration (%)	Retention Time (RT)
2,2-Dimethoxybutane (C ₆ H ₁₄ O ₂) M.W. = 118.176 g/mol		1.02	3.591	0.84	3.593
Dimethyl 2-methoxybutanedioate (C ₇ H ₁₂ O ₅) M.W. = 176.168 g/mol		1.38	17.695	1.77	17.7
5-(hydroxymethyl)furan-2-carbaldehyde (C ₆ H ₆ O ₃) M.W. = 126.111 g/mol		3.81	22.128	2.71	22.272
2,3-Dihydroxypropyl acetate (C ₅ H ₁₀ O ₄) M.W. = 134.131 g/mol		4.80	22.816	2.31	22.822
2-(Hydroxymethyl)-2-nitropropane-1,3-diol (C ₄ H ₉ NO ₅) M.W. = 151.118 g/mol		2.96	32.96	1.68	33.065
Dimethyl benzene-1,4-dicarboxylate (C ₁₀ H ₁₀ O ₄) M.W. = 194.186 g/mol		3.67	34.828	4.66	34.838
Methyl hexadecanoate (C ₁₇ H ₃₄ O ₂) M.W. = 270.457 g/mol		0.98	50.078	1.24	50.088
Methyl 3-(3,5-ditert-butyl-4-hydroxyphenyl)propanoate (C ₁₈ H ₂₈ O ₃) M.W. = 292.419 g/mol		9.00	50.385	10.31	50.398
Hexadecanoic acid C ₁₆ H ₃₂ O ₂ M.W. = 256.43 g/mol		3.62	51.423	2.30	51.424

(continued on next page)

Table 1 (continued)

Metabolites	Structure	Healthy roots		<i>G. boninense</i> infected roots	
		Concentration (%)	Retention Time (RT)	Concentration (%)	Retention Time (RT)
Methyl (9Z,12Z)-octadeca-9,12-dienoate (C ₁₉ H ₃₄ O ₂) M.W. = 294.479 g/mol		0.77	55.679	1.27	55.688
Methyl (Z)-octadec-6-enoate (C ₁₉ H ₃₆ O ₂) M.W. = 296.495 g/mol		1.25	55.866	1.79	55.88
Methyl octadecanoate (C ₁₉ H ₃₈ O ₂) M.W. = 298.511 g/mol		0.80	56.683	1.08	56.691
(E)-icos-5-ene (C ₂₀ H ₄₀) M.W. = 280.54 g/mol		0.85	57.892	0.58	57.901
Stigmasterol (C ₂₉ H ₄₈ O) M.W. = 412.702 g/mol		1.65	86.22	1.55	86.233
Stigmast-5-en-3-ol, (3β) (C ₂₉ H ₅₀ O) M.W. = 414.718 g/mol		4.53	87.909	5.23	87.933

*M.W. - molecular weight.

2.2. GC-MS and data analysis

The solvent-free root extracts of non-infected and *G. boninense* infected oil palm were dissolved in HPLC-grade methanol. The samples were analyzed using gas chromatography equipped with mass spectrometry (GC-MS-2010 Plus-Shimadzu). The column temperature was set to 50 °C (4 min), then increased to 320 °C at the rate of 7 °C/min, and then held for 20 min. The injector temperature was set at 280 °C (split mode = 20:1; injection volume = 0.1 μL). The flow rate of the helium carrier gas was set to 1 mL/min (total run time = 60 min). Mass spectra were set from the range *m/z* 40 to 700 whereas the electron ionization at 70 eV. The chromatograms of the sample were examined by comparing their mass spectra with the database

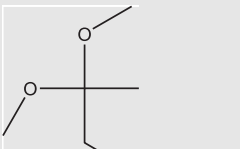
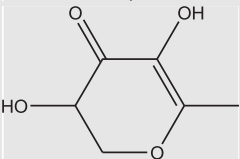
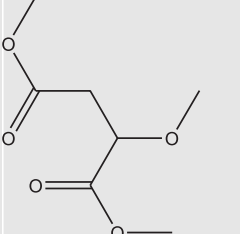
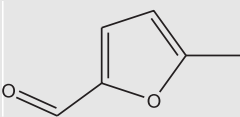
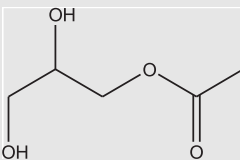
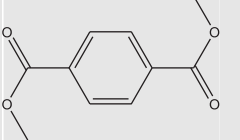
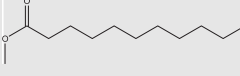
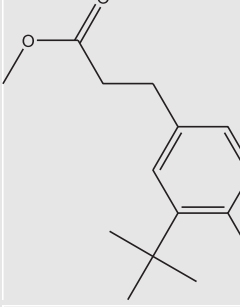
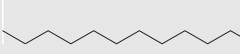
library of National Institute of Standards and Technology (NIST11). The GC-MS chromatograms were aligned using The XCMS package in R version 2.13.0. PCA using scaling based on Variance was analyzed by SIMCA 13.0 software.

3. Results and discussion

3.1. GC-MS analysis and metabolites identification

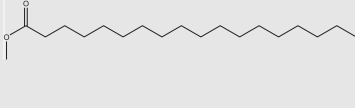
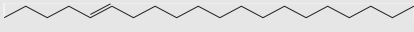
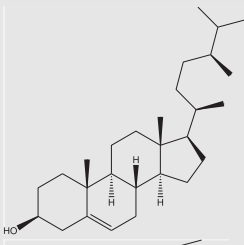
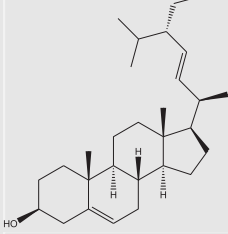
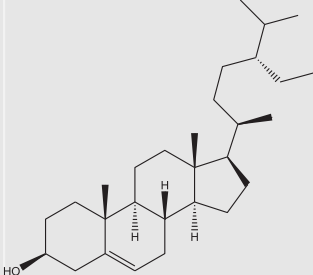
The GC-MS analysis of 80% (v/v) methanol crude extracts resulted in identification of 15 metabolites in non-infected roots (control of 14 days post-infection) and *G. boninense* infected roots at 14 days post-infection whereas 14 metabolites were identified in non-infected roots (control of 30 days

Table 2 Chemical composition of healthy roots (control of 30 days-post infection) and *G. boninense* infected roots at 30 days-post infection.

Metabolites	Structure	Healthy roots		<i>G. boninense</i> infected roots	
		Concentration (%)	Retention Time (RT)	Concentration (%)	Retention Time (RT)
2,2-Dimethoxybutane (C ₆ H ₁₄ O ₂) M.W. = 118.176 g/mol		1.27	3.589	0.97	3.584
3,5-Dihydroxy-6-methyl-2,3-dihydropyran-4-one (C ₆ H ₈ O ₄) M.W. = 144.126 g/mol		5.28	17.802	1.77	17.78
Dimethyl 2-methoxybutanedioate (C ₇ H ₁₂ O ₅) M.W. = 176.168 g/mol		1.01	21.86	1.27	21.889
5-(Hydroxymethyl)furan-2-carbaldehyde (C ₆ H ₆ O ₃) M.W. = 126.111 g/mol		9.83	22.158	1.19	22.15
2,3-dihydroxypropyl acetate (C ₅ H ₁₀ O ₄) M.W. = 134.131 g/mol		5.83	22.818	3.21	22.806
Dimethyl benzene-1,4-dicarboxylate (C ₁₀ H ₁₀ O ₄) M.W. = 194.186 g/mol		2.94	34.809	3.98	34.808
Methyl hexadecanoate (C ₁₇ H ₃₄ O ₂) M.W. = 270.457 g/mol		0.96	50.05	1.10	50.047
Methyl 3-(3,5-ditert-butyl-4-hydroxyphenyl)propanoate (C ₁₈ H ₂₈ O ₃) M.W. = 292.419 g/mol		6.69	50.35	10.47	50.359
Hexadecanoic acid (C ₁₆ H ₃₂ O ₂) M.W. = 256.43 g/mol		5.70	51.397	2.21	51.388

(continued on next page)

Table 2 (continued)

Metabolites	Structure	Healthy roots		<i>G. boninense</i> infected roots	
		Concentration (%)	Retention Time (RT)	Concentration (%)	Retention Time (RT)
Methyl (<i>Z</i>)-octadec-6-enoate (C ₁₉ H ₃₆ O ₂) M.W. = 296.495 g/mol		0.95	55.856	1.96	55.837
Methyl octadecanoate (C ₁₉ H ₃₈ O ₂) M.W. = 298.511 g/mol		0.67	56.644	1.21	56.65
(<i>E</i>)-Icos-5-ene (C ₂₀ H ₄₀) M.W. = 280.54 g/mol		1.32	57.868	0.51	57.859
Ergost-5-en-3-ol, (3β) (C ₂₈ H ₄₈ O) M.W. = 400.691 g/mol		Notdetected	Not detected	1.97	85.565
Stigmasterol (C ₂₉ H ₄₈ O) M.W. = 412.702 g/mol		2.87	86.165	2.07	86.162
Stigmast-5-en-3-ol, (3β) (C ₂₉ H ₅₀ O) M.W. = 414.718 g/mol		6.59	87.853	5.26	87.853

*M.W. - molecular weight

post-infection) and 15 metabolites were identified in *G. boninense* infected roots at 30 days post-infection.

The metabolites and the percentage values of composition of metabolites present in non-infected roots (control of 14 days post-infection) are shown in Table 1. The obtained results indicated that the main compounds were 2,2-dimethoxybutane (1.02%), dimethyl 2-methoxybutanedioate (1.38%), 5-(hydroxymethyl)furan-2-carbaldehyde (3.81%), 2,3-dihydroxypropyl acetate (4.80%), 2-(hydroxymethyl)-2-nitropropane-1,3-diol (2.96%), dimethyl benzene-1,4-dicarboxylate (3.67%), methyl hexadecanoate (0.98%), methyl 3-(3,5-ditert-butyl-4-hydroxyphenyl)propanoate (9.00%), hexadecanoic acid (3.62%), methyl (9*Z*,12*Z*)-octadeca-9,12-dienoate (0.77%), methyl (*Z*)-octadec-6-enoate (1.25%), methyl octadecanoate (0.80%),

(*E*)-icos-5-ene (0.85%), stigmasterol (1.65%) and stigmast-5-en-3-ol, (3β) (4.53%).

The metabolites that were characterized in *G. boninense* infected roots (14 days post-infection) (Table 1) were 2,2-dimethoxybutane (0.84%), dimethyl 2-methoxybutanedioate (1.77%), 5-(hydroxymethyl)furan-2-carbaldehyde (2.71%), 2,3-dihydroxypropyl acetate (2.31%), 2-(hydroxymethyl)-2-nitropropane-1,3-diol (1.68%), dimethyl benzene-1,4-dicarboxylate (4.66%), methyl hexadecanoate (1.24%), methyl 3-(3,5-ditert-butyl-4-hydroxyphenyl)propanoate (10.31%), hexadecanoic acid (2.30%), methyl (9*Z*,12*Z*)-octadeca-9,12-dienoate (1.27%), methyl (*Z*)-octadec-6-enoate (1.79%), methyl octadecanoate (1.08%), (*E*)-icos-5-ene (0.58%), stigmasterol (1.55%) and stigmast-5-en-3-ol, (3β) (5.23%).

The metabolites in non-infected roots (control of 30 days post-infection) were identified (Table 2) as 2,2-dimethoxybutane (1.27%), 3,5-dihydroxy-6-methyl-2,3-dihydropyran-4-one (5.28%), dimethyl 2-methoxybutanedioate (1.01%), 5-(hydroxymethyl)furan-2-carbaldehyde (9.83%), 2,3-dihydroxypropyl acetate (5.83%), dimethyl benzene-1,4-dicarboxylate (2.94%), methyl hexadecanoate (0.96%), methyl 3-(3,5-ditert-butyl-4-hydroxyphenyl)propanoate (6.69%), hexadecanoic acid (5.70%), methyl (*Z*)-octadec-6-enoate (0.95%), methyl octadecanoate (0.67%), (*E*)-icos-5-ene (1.32%), stigmasterol (2.87%) and stigmast-5-en-3-ol, (3 β) (6.59%).

The *G. boninense* infected roots (30 days post-infection) contains 15 metabolites (Table 2) such as 2,2-dimethoxybutane (0.97%), 3,5-dihydroxy-6-methyl-2,3-dihydropyran-4-one (1.77%), dimethyl 2-methoxybutanedioate (1.27%), 5-(hydroxymethyl)furan-2-carbaldehyde (1.19%), 2,3-dihydroxypropyl acetate (3.21%), dimethyl benzene-1,4-dicarboxylate (3.98%), methyl hexadecanoate (1.10%), methyl 3-(3,5-ditert-butyl-4-hydroxyphenyl)propanoate (10.47%), hexadecanoic acid (2.21%), methyl (*Z*)-octadec-6-enoate (1.96%), methyl octadecanoate (1.21%), (*E*)-icos-5-ene (0.51%), ergost-5-en-3-ol, (3 β) (1.97%), stigmasterol (2.07%) and stigmast-5-en-3-ol, (3 β) (5.26%).

PCA was applied to understand the clustering features of the non-infected and infected sample and the metabolites contributing to the variability. A three-component model was generated with goodness of fit [$R^2X(\text{cum})$ of 0.895 and $Q^2(\text{cum})$ of = 0.393] and the first two principal component (PC1 and PC2) explaining 79.2%. A score plot was constructed using PC1 and PC2 [$R^2X(\text{cum})$ of 0.792 and $Q^2(\text{cum})$ of = 0.719; with 95% confidence level], showing two clear separated clusters were identified by PC1 without any notable outliers (Fig. 1).

In identifying the root extract metabolites responsible for each differentiation, PCA models were generated in loading bi-pot (Fig. 2). 3,5-dihydroxy-6-methyl-2,3-dihydropyran-4-one, dimethyl 2-methoxybutanedioate, 5-(hydroxymethyl)fura

n-2-carbaldehyde, 2,3-dihydroxypropyl acetate and hexadecanoic acid were found higher in non-infected roots whereas 2,2-dimethoxybutane, dimethyl benzene-1,4-dicarboxylate, methyl hexadecanoate, methyl 3-(3,5-ditert-butyl-4-hydroxyphenyl)propanoate, methyl (*Z*)-octadec-6-enoate, methyl octadecanoate, (*E*)-Icos-5-ene, 2-(hydroxymethyl)-2-nitropropane-1,3-diol, stigmasterol, stigmast-5-en-3-ol, (3 β), ergost-5-en-3-ol, (3 β) and methyl (9*Z*,12*Z*)-octadeca-9,12-dienoate were found more abundant in infected roots.

Fatty acids has been known as essential macromolecules exist in all living organisms which are composed of carboxylic acids attached to hydrocarbon chains. Saturated fatty acids can be defined as a compound in which hydrogen molecules occupy all bonding positions between the carbons, whereas unsaturated fatty acids contain one or more double bonds between their carbons. Different fatty acids can be identified by the length of their carbon chain and the number of double bonds between the carbons. Fatty acids and their methyl esters regulate a variety of responses to biotic and abiotic stresses in plant (Kachroo and Kachroo, 2009; McFarlane 1968).

Previous study reported that, fatty acids and their methyl esters such as methyl hexadecanoate, methyl octadecanoate, methyl (9*Z*,12*Z*)-octadeca-9,12-dienoate, dimethyl benzene-1,4-dicarboxylate, methyl (*Z*)-octadec-6-enoate, methyl 3-(3,5-ditert-butyl-4-hydroxyphenyl)propanoate and 5-eicosene could be acting as potent antimicrobial agent against pathogen (Akpuaka et al., 2013; Bashir et al., 2012; Pu et al., 2010; Rozlianah et al., 2015). This can be indicated that, the abundance of these fatty acids and their methyl esters in *G. boninense* infected roots are due to the crucial roles in pathogen defence (Varns & Glynn, 1979; Alexander et al., 2017).

The highest concentration of the steroidal compounds in the *G. boninense* infected samples such as stigmasterol, stigmast-5-en-3-ol, (3 β) and ergost-5-en-3-ol, (3 β) in *G. boninense* infected samples are related to the act as plant defense metabolites apart from performing as plant growth regulators (Faure et al., 2009) and controlling the fluidity of plant membranes for alteration to changes in temperature (Piironen et al.,

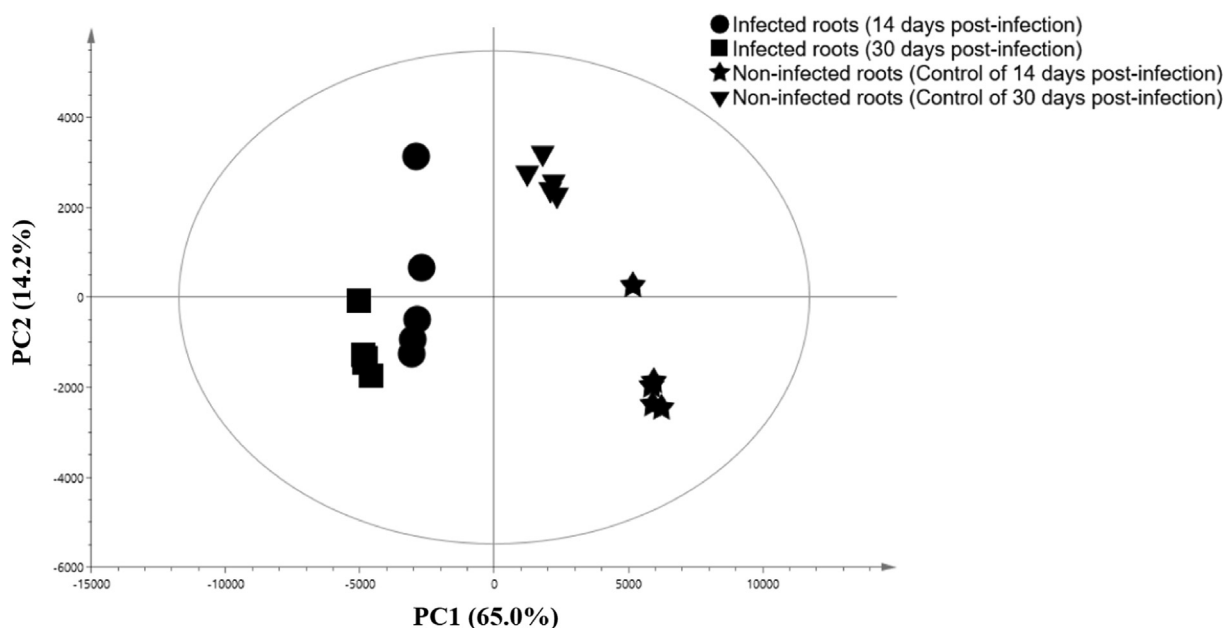


Fig. 1 PCA score plots derived from the GC–MS chromatogram of healthy and *G. boninense* infected roots.

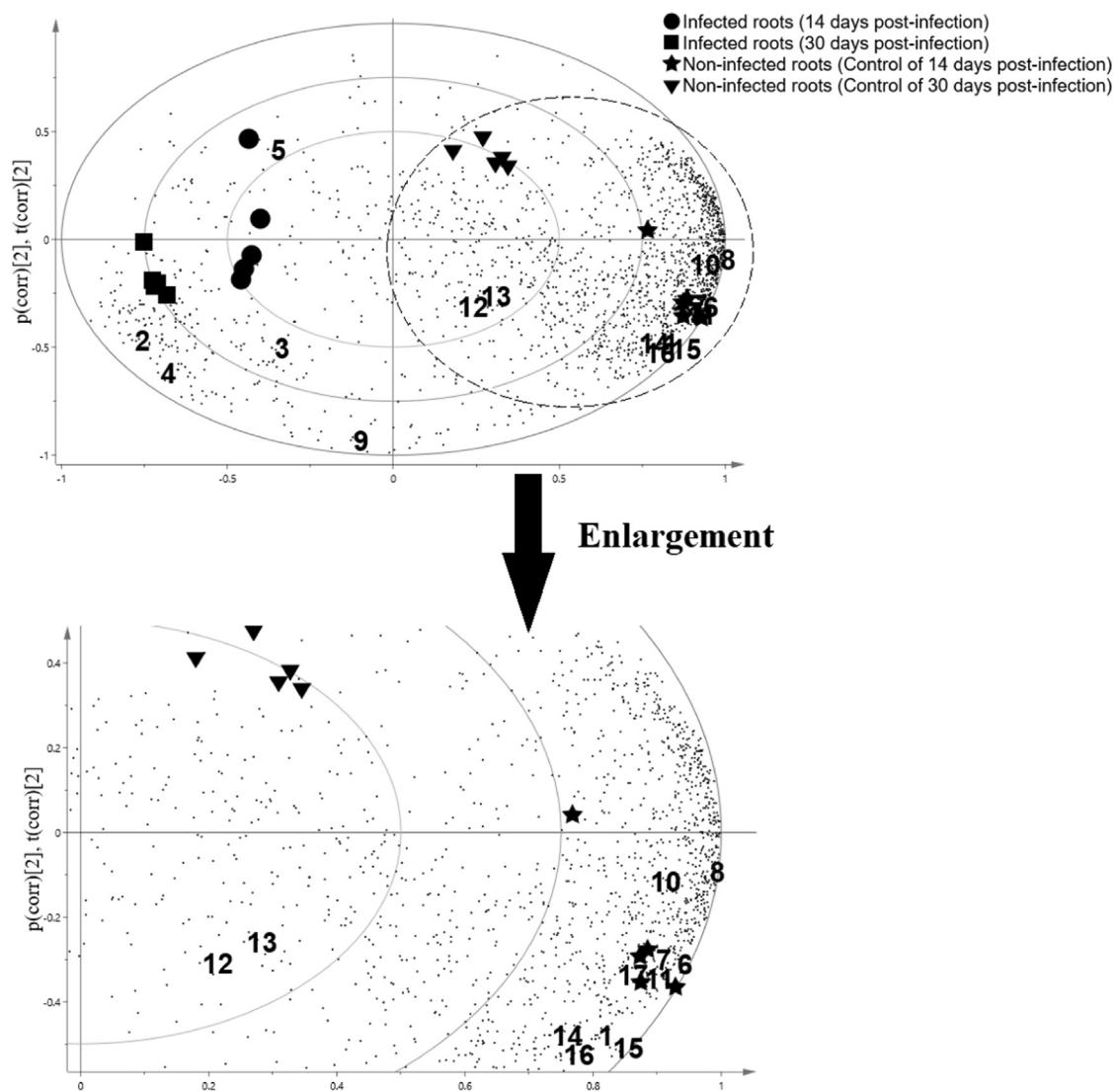


Fig. 2 The PCA loadings bi-plot of the target compounds in oil palm roots and their correlation to the healthy and *G. boninense* infected. Abbreviations: 1: 2,2-Dimethoxybutane; 2: 3,5-Dihydroxy-6-methyl-2,3-dihydropyran-4-one; 3: Dimethyl 2-methoxybutanedioate; 4: 5-(Hydroxymethyl)furan-2-carbaldehyde; 5: 2,3-dihydroxypropyl acetate; 6: Dimethyl benzene-1,4-dicarboxylate; 7: Methyl hexadecanoate; 8: Methyl 3-(3,5-ditert-butyl-4-hydroxyphenyl)propanoate; 9: Hexadecanoic acid; 10: Methyl (*Z*)-octadec-6-enoate; 11: Methyl octadecanoate; 12: (*E*)-Icos-5-ene; 13: 2-(Hydroxymethyl)-2-nitropropane-1,3-diol; 14: Stigmasterol; 15: Stigmast-5-en-3-ol, (3β); 16: Ergost-5-en-3-ol, (3β); 17: Methyl (9*Z*,12*Z*)-octadeca-9,12-dienoate.

2000). The plant cell triggered plant defense response during the pathogen attack and embarks signaling events leading to increase expression of genes involved in sterol biosynthesis, leading to induction of stigmasterol (Fig. 3) (Wang et al., 2012; Aboobucker & Suza, 2019).

Stigmasterol is produced via the mevalonate pathway following a series of enzyme-catalyzed reactions leading to the generation of 2,3-oxidosqualene (Schaller, 2003; Bach, 2016). This is followed by conversion of 2,3-oxidosqualene to cycloartenol by cycloartenol synthase (Benveniste, 2004; Griebel and Zeier, 2010; Gas-Pascual et al., 2014; Sonawane et al., 2016). Two phytosterol biosynthetic pathways has been identified by (Ohyama et al., 2009) after they identified lanosterol synthase 1 in *Arabidopsis*. The major part of the metabolic flux occurs via cycloartenol whereas a minor part takes place via LAS1 and lanosterol. Several enzymatic steps such as methyl

transferases, reductases, isomerases, demethylases and desaturases are needed to convert cycloartenol or lanosterol to stigmasterol or lanosterol to stigmasterol (Schaller, 2004). Subsequently, stigmasterol-5-en-3-ol or known as β -sitosterol is converted to stigmasterol by the cytochrome P450 CYP710A1 via C22 desaturation (Griebel and Zeier, 2010).

Ergost-5-en-3-ol, (3β) or known as campesterol has been reported to be produced from 24-methylenecycloartenol in which 24-methylenecycloartenol is converted to 24-methylenecholesterol through several steps (Fig. 3). Then it is epimerized to 24-methylidestosterol followed by hydrogenation of the epimerized double bond to produce campesterol (Yokota, 1999). The production of these steroidal compounds that is triggered after pathogen infection could be suggested the higher level of stigmasterol and stigmasterol-5-en-3-ol in *G. boninense* infected roots.

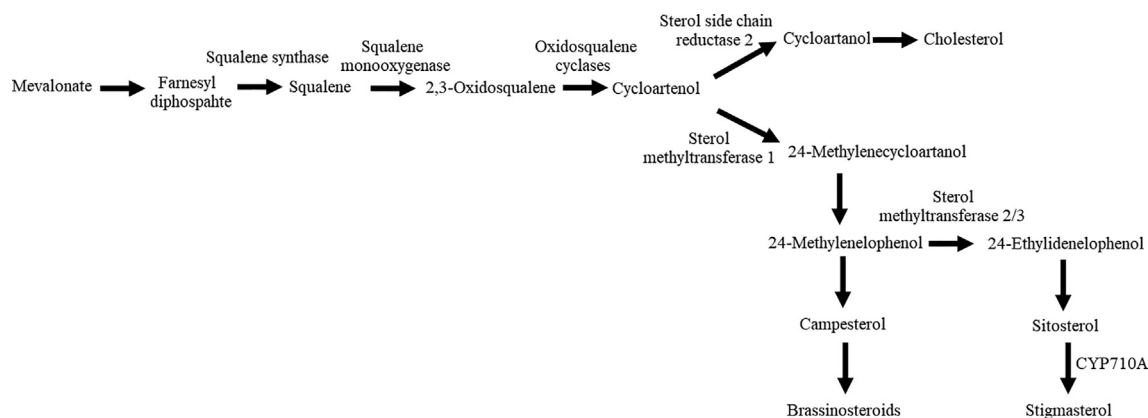


Fig. 3 Biosynthetic pathway for plant sterols. Modified from Wang et al., 2012 and Aboobucker and Suza, 2019.

4. Conclusion

The results showed that GC–MS chromatogram of non-infected and *G. boninense* infected roots (14 and 30 day post-infection) exhibited differences which were discriminated and clustered into groups through multivariate data analysis of PCA. Steroidal compounds (stigmasterol, stigmasterol-5-en-3-ol, (3 β) and ergost-5-en-3-ol, (3 β)) and fatty acid derivatives (methyl hexadecanoate, methyl octadecanoate, methyl (9Z,12Z)-octadeca-9,12-dienoate, dimethyl benzene-1,4-dicarboxylate, methyl (Z)-octadec-6-enoate, methyl 3-(3,5-ditert-butyl-4-hydroxyphenyl)propanoate and 5-eicosene) which has been found more abundant in the *G. boninense* infected oil palm roots could be used as chemical marker for early detection of basal stem rot disease in oil palm in the future since there is no single chemical marker that could serve as marker in detection of *G. boninense*.

Declaration of Competing Interest

The author declare that there is no conflict of interest.

Acknowledgements

This work was supported by Ministry of Higher Education Malaysia, Long Term Research Grant Schemes (LRGS)-Nanomite and Universiti Putra Malaysia [grant numbers 5526301, 5526304, 9443101 & 9443104].

References

- Aboobucker, S.I., Suza, W.P., 2019. Why do plants convert sitosterol to stigmasterol?. *Front. Plant Sci.* 10 (354), 1–8. <https://doi.org/10.3389/fpls.2019.00354>.
- Akpuaka, A., Ekwenchi, M.M., Dashak, D.A., Dildar, A., 2013. Biological activities of characterized isolates of n-hexane extract of *Azadirachta Indica* A. Juss (Neem) leaves. *Nat. Sci.* 11 (5), 141–147.
- Bach, T.J., 2016. Secondary metabolism: high cholesterol in tomato. *Nat. Plants* 3, 16213. <https://doi.org/10.1038/nplants.2016.213>.
- Bashir, A., Ibrar, K., Shumaila, B., Azam, S.J., 2012. Chemical composition and antifungal, phytotoxic, brine shrimp cytotoxicity, insecticidal and antibacterial activities of the essential oils of *Acacia modesta*. *J. Med. Plants Res.* 6 (31), 4653–4659. <https://doi.org/10.5897/JMPR12.016>.
- Alexander, A., Dayou, J., Abdullah, S., Chong, K.P., 2017. The changes of oil palm roots cell wall lipids during pathogenesis of *Ganoderma boninense*. *IOP Conf. Ser. Earth Sci.* 77, 012014.
- Benveniste, P., 2004. Biosynthesis and accumulation of sterols. *Annu. Rev. Plant Biol.* 55, 429–457. <https://doi.org/10.1146/annurev.arplant.55.031903.141616>.
- Durak, H., Genel, S., 2020. Catalytic Hydrothermal Liquefaction of *Lactuca scariola* with a heterogeneous catalyst: the investigation of temperature, reaction time and synergistic effect of catalysts. *Bioresour. Technol.* 309, . <https://doi.org/10.1016/j.biortech.2020.123375> 123375.
- Durak, H., Genel, S., Tunç, M., 2019. Pyrolysis of black cumin seed: Significance of catalyst and temperature product yields and chromatographic characterization. *J. Liq. Chromatogr. Relat. Technol.* 42 (11–12), 331–350. <https://doi.org/10.1080/10826076.2019.1593194>.
- Faure, D., Vereecke, D., Leveau, J.H.J., 2009. Molecular communication in the rhizosphere. *Plant Soil* 321, 279–303.
- Flood, J., Hasan, Y., Foster, H., 2002. *Ganoderma* diseases of oil palm—an interpretation from Bah Lias Research Station. *Planter* 78, 689–710.
- Gas-Pascual, E., Berna, A., Bach, T.J., Schaller, H., 2014. Plant oxidosqualene metabolism: cycloartenol synthase-dependent sterol biosynthesis in *Nicotiana benthamiana*. *PLoS One* 9, <https://doi.org/10.1371/journal.pone.0109156> e109156.
- Griebel, T., Zeier, J., 2010. A role for β -sitosterol to stigmasterol conversion in plant–pathogen interactions. *Plant J.* 63 (2), 254–268. <https://doi.org/10.1111/j.1365-313X.2010.04235.x>.
- Hu, Z., Chang, X., Dai, T., Li, L., Liu, P., Wang, G., Liu, P., Huang, Z., Liu, X., 2019. Metabolic Profiling to Identify the Latent Infection of Strawberry by *Botrytis cinerea*. *Evolutionary Bioinformatics* 15, 1–7. <https://doi.org/10.1177/1176934319838518>.
- Hushiaran, R., Yusof, N.A., Dutse, S.W., 2013. Detection and control of *Ganoderma boninense*: strategies and perspectives. *SpringerPlus* 2 (555), 1–12. <https://doi.org/10.1186/2193-1801-2-555>.
- Idris, A.S., Kushairi, A., Ariffin, D., Basri, M.W., 2006. **Technique for inoculation of oil palm geminated seeds with *Ganoderma***. *MPOB Inf. Ser.* 314, 1.
- Isha, A., Akanbi, F.S., Yusof, N.A., Osman, R., Wong, M.Y., Abdullah, S.N.A., 2019. An NMR metabolomics approach and detection of *Ganoderma boninense*-infected oil palm leaves using MWCNT-based electrochemical sensor. *J. Nanomater.* 2019. <https://doi.org/10.1155/2019/4729706> 4729706.
- Kachroo, A., Kachroo, P., 2009. Fatty Acid-derived signals in plant defense. *Annu. Rev. Phytopathol.* 47, 153–176. <https://doi.org/10.1146/annurev-phyto-080508-081820>.
- Karre, S., Kumar, A., Dhokane, D., Kushalappa, A.C., 2017. Metabolo-transcriptome profiling of barley reveals induction of chitin elicitor receptor kinase gene (HvCERK1) conferring resis-

- tance against *Fusarium graminearum*. *Plant Mol. Biol.* 93, 247–267. <https://doi.org/10.1007/s11103-016-0559-3>.
- Kumar, A., Yogendra, K.N., Karre, S., Kushalappa, A.C., Dion, Y., Choo, T.M., 2016. WAX INDUCER1 (HvWIN1) transcription factor regulates free fatty acid biosynthetic genes to reinforce cuticle to resist *Fusarium* head blight in barley spikelets. *J. Exp. Bot.* 67, 4127–4139. <https://doi.org/10.1093/jxb/erw187>.
- McFarlane, J.E., 1968. Fatty acids, methyl esters and insect growth. *Comp. Biochem. Physiol.* 24 (2), 377–384. [https://doi.org/10.1016/0010-406x\(68\)90989-4](https://doi.org/10.1016/0010-406x(68)90989-4).
- Muniroh, M.S., Nusbah, S.A., Vadmalai, G., Siddique, Y., 2019. Proficiency of biocontrol agents as plant growth promoters and hydrolytic enzymes producers in *Ganoderma boninense* infected oil palm seedlings. *Curr. Plant Biol.* 20, <https://doi.org/10.1016/j.cpb.2019.100116> 100116.
- Pu, Z.H., Zhang, Y.Q., Yin, Z.Q., Xu, J., Jia, R.Y., Lu, Y., Yang, F., 2010. Antibacterial activity of 9-octadecanoic acid-hexadecanoic acid-tetrahydrofuran-3,4-diyester from neem oil. *Agr. Sci. China* 9 (8), 1236–1240. [https://doi.org/10.1016/S1671-2927\(09\)60212-1](https://doi.org/10.1016/S1671-2927(09)60212-1).
- Ohyama, K., Suzuki, M., Kikuchi, J., Saito, K., Muranaka, T., 2009. Dual biosynthetic pathways to phytosterol via cycloartenol and lanosterol in *Arabidopsis*. *Proc Natl Acad Sci USA* 106 (3), 725–730. <https://doi.org/10.1073/pnas.0807675106>.
- Piironen, V., Lindsay, D.G., Miettinen, T.A., Toivo, J., Lampi, A.M., 2000. Plant sterols: biosynthesis, biological function and their importance to human nutrition. *J. Sci. Food Agric.* 80, 939–966. [https://doi.org/10.1002/\(SICI\)1097-0010\(20000515\)80:7<939::AID-JSFA644>3.0.CO;2-C](https://doi.org/10.1002/(SICI)1097-0010(20000515)80:7<939::AID-JSFA644>3.0.CO;2-C).
- Rozali, N.L., Yarmo, M.A., Idris, A.S., Kushiari, A., Ramli, U.S., 2017. Metabolomics differentiation of oil palm (*Elaeis guineensis* Jacq.) spear leaf with contrasting susceptibility to *Ganoderma boninense*. *Plant Omics J.* 10 (2), 45–52. <https://doi.org/10.21475/poj.10.02.17.pne364>.
- Rozlianah, F.S., Jualang, A.G., Chong, K.P., 2015. Fatty acids and phenols involved in resistance of oil palm to *Ganoderma boninense*. *Adv. Environ. Biol.* 9 (2), 11–16.
- Schaller, H., 2003. The role of sterols in plant growth and development. *Prog. Lipid Res.* 42 (3), 163–175. [https://doi.org/10.1016/S0163-7827\(02\)00047-4](https://doi.org/10.1016/S0163-7827(02)00047-4).
- Schaller, H., 2004. New aspects of sterol biosynthesis in growth and development of higher plants. *Plant Physiol. Biochem.* 42, 465–476. <https://doi.org/10.1016/j.plaphy.2004.05.01>.
- Sonawane, P.D., Pollier, J., Panda, S., Szymanski, J., Massalha, H., Yona, M., et al, 2016. Plant cholesterol biosynthetic pathway overlaps with phytosterol metabolism. *Nat. Plants* 3, 16205. <https://doi.org/10.1038/nplants.2016.205>.
- Susanto, A., Sudharto, P.S., Purba, R.Y., 2005. Enhancing biological control of basal stem rot disease (*Ganoderma boninense*) in oil palm plantations. *Mycopathologia* 159 (1), 153–157. <https://doi.org/10.1007/s11046-004-4438-0>.
- Varns, J.L., Glynn, M.T., 1979. Detection of disease in stored potatoes by volatile monitoring. *Am. Potato J.* 56, 185–197. <https://doi.org/10.1007/BF02853365>.
- Wang, K., Senthil-Kumar, M., Ryu, C.M., Kang, L., Mysore, K.S., 2012. Phytosterols play a key role in plant innate immunity against bacterial pathogens by regulating nutrient efflux into the apoplast. *Plant Physiol.* 158 (4), 1789–1802. <https://doi.org/10.1104/pp.111.189217>.
- Yogendra, K.N., Kumar, A., Sarkar, K., Li, Y., Pushpa, D., Mosa, K. A., Duggavathi, R., Kushalappa, A.C., 2015. Transcription factor StWRKY1 regulates phenylpropanoid metabolites conferring late blight resistance in potato. *J. Exp. Bot.* 66, 7377–7389. <https://doi.org/10.1093/jxb/erv434>.
- Yokota, T., 1999. *Brassinosteroids in Hooykass P.J.J., Hall M.A., Libbenga K.R. (Eds.), Biochemistry and Molecular Biology of Plant Hormones. Elsevier Science, London, pp. 277-29.*
- Zain, N., Seman, I.A., Kushairi, A., Ramli, U.S., 2013. Metabolite profiling of oil palm towards understanding basal stem rot (BSR) disease. *J. Oil Palm. Res.* 25 (1), 58–71.
- Zhou, Y., Qin, D.Q., Zhang, P.W., Chen, X.T., Liu, B.J., Cheng, D. M., Zhang, Z.X., 2020. Integrated LC–MS and GC–MS-based untargeted metabolomics studies of the effect of azadirachtin on *Bactrocera dorsalis* larvae. *Sci. Rep.* 10, 1–11. <https://doi.org/10.1038/s41598-020-58796-9>.